A Dynamic Human Reliability Analysis Approach Using Continuous Markov Chain Monte Carlo Method: Formulation of a Computational Framework for Responding to Environmental Spatiotemporal Changes

Chun-Yen Li [1*], Yukihiro Kirimoto [1]

[1] *Central Research Institute of Electric Power Industry: 2-6-1 Nagasaka, Yokosuka, Kanagawa, 240-0196, li40806@criepi.denken.or.jp*

ABSTRACT

Advancing Human Reliability Analysis (HRA) is vital for nuclear safety, as it evaluates human responses to accidents within Probabilistic Risk Assessment (PRA) Conventional HRA methods estimate Human Error Probability (HEP) based on Performance Shaping Factors (PSFs) under static scenarios but struggle to address dynamic environmental changes. To overcome this limitation, it is crucial to model uncertainties in human behavior arising from continuously evolving spatiotemporal environmental conditions. This research aims to develop a dynamic HRA approach that incorporates the effects of evolving environments on human behavior. To achieve this, we propose a computational framework that utilizes the Continuous Markov Chain Monte Carlo (CMMC) method. Within this framework, PSFs are regularly updated based on monitored environmental changes to capture their impact on HEP. Subsequently, Monte Carlo sampling is employed to generate stochastic human behavior events, which in turn provide feedback to the environment. Through this iterative process, a dynamic HRA approach is realized by fostering evolving, bidirectional interactions between humans and their surrounding environment. A hypothetical example applying this proposed computational framework is also demonstrated in this research, showcasing its potential to quantitively confirm the previously unexplored influence on the repair task resulted from dynamic phenomenon.

Keywords: Dynamic human reliability analysis, Continuous Markov chain Monte Carlo method, Dynamic interaction between human and environments, Performance shaping factors, Human error probability.

I. INTRODUCTION

Probabilistic Risk Assessment (PRA) serves as a fundamental approach for addressing the intricate safety and reliability issues within Nuclear Power Plants (NPPs). A key part of PRA is Human Reliability Analysis (HRA), which focuses on detecting potential human errors and quantifying their likelihood, known as Human Error Probability (HEP), during safety evaluations. Among the many HRA techniques developed over time, the Technique for Human Error Rate Prediction (THERP) is particularly prominent [1]. THERP analyzes a target task by breaking it down into smaller, discrete steps using a decision tree model, while incorporating Performance Shaping Factors (PSFs) that represent external environmental conditions and internal operator characteristics such as skill level.

However, traditional HRA methods generally depend on fixed, static scenarios, making them inadequate for capturing how transient environmental variations affect operator performance. This limitation results in persistent uncertainties when assessing dynamic accident scenarios. Furthermore, dynamic PRA approaches have been developed to explicitly model the timing and sequence of events, thus providing a more thorough identification of failure paths throughout different accident progressions. This evolving research trend underscores the urgent need for dynamic HRA methodologies that can effectively account for fluctuating environmental influences on human tasks and integrate smoothly within dynamic PRA frameworks.

This paper aims to develop a dynamic HRA approach that reflects changing environmental impacts on human behavior over time. The approach extends conventional HRA by utilizing the Continuous Markov Chain Monte Carlo (CMMC) method [2], which has been previously applied in dynamic PRA analyses. In this approach, the Markov chain process continuously updates PSFs based on real-time environmental monitoring, thereby influencing the estimation of HEP. These updated probabilities then guide Monte Carlo simulations that generate stochastic sequences of dynamic events. Additionally, an originally proposed computational framework is introduced in this research, designed to capture the mutual interactions

between humans and their environment in a cyclic manner. An example is also presented in this study to illustrate how the proposed framework leverages the CMMC method to enhance the flexibility of the traditional HRA approach.

II. METHODOLOGY

II.A. Computational Framework Overview

The proposed dynamic analysis framework, as shown in Fig. 1, is built upon two key components: (1) the Structures, Systems, and Components (SSCs) State Solver, which functions based on stochastic principles, and (2) the Plant State Solver, which operates deterministically.

After initializing all the necessary parameters, the SSCs State Solver is activated firstly, processing the current SSCs and plant information through either the Malfunction Analysis Module or Repair Analysis Module, depending on whether the specific j_{th} SSC (SSC_j^n, n is the current step in the analysis framework) is presently functioning or malfunctioning. Subsequently, CMMC method is applied with referring to the plant conditions to update the SSC state stochastically from SSC_j^n to SSC_j^{n+1}. Until all the SSC_j^ns are evaluated, the framework transfers all the updated SSCs states to the Plant State Solver.

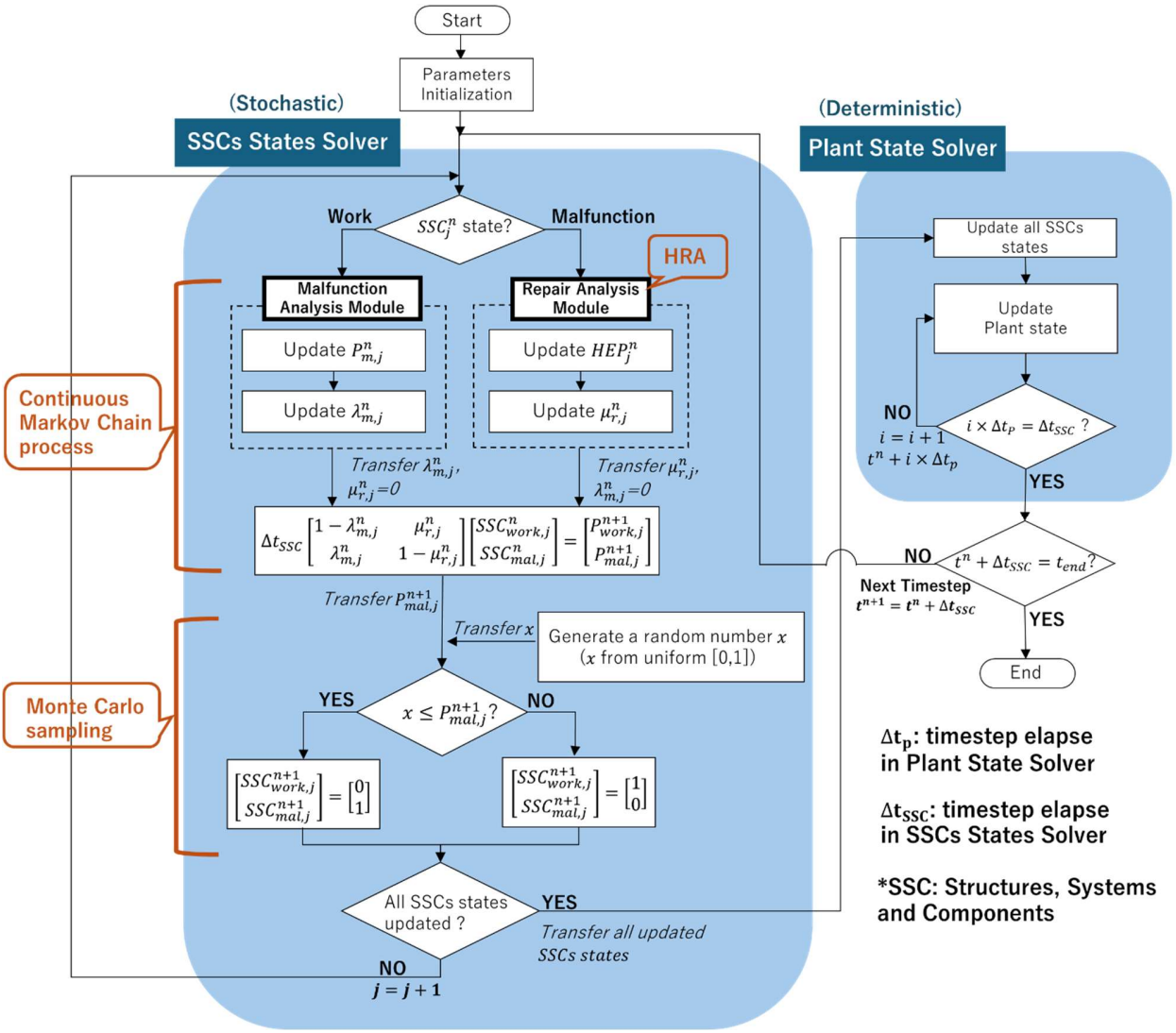

FIGURE 1. The proposed CMMC-based framework.

Following which, the Plant State Solver then conducts transient analyses (such as Computational Fluid Dynamics simulations) to model the plant state deterministically. After completing the transient analysis, if the predetermined end time (t_{end}) has not been reached yet, the updated plant state information is transferred to the SSCs State Solver.

Ultimately, this framework creates a dynamic, bidirectional coupling analysis that combines deterministic environmental simulations with stochastic modeling of SSC behaviors in a cyclical manner. Since the previous research [2] covers the CMMC method's application to SSC malfunction analysis, the next section will explore how to use CMMC method for dynamic repair analysis, particularly focusing on expanding traditional HRA into a dynamic framework.

II.B. Utilizing CMMC Method to Dynamically Embed HRA in the Framework

The use of the CMMC method within the SSCs State Solver can be divided into two main components: (1) the continuous Markov chain process and (2) Monte Carlo sampling, as depicted in Fig. 1. During the continuous Markov chain process, if the Repair Analysis Module is enabled, HRA is carried out to estimate the HEP for the repair task of the j_{th} SSC at the n_{th} step (HEP_j^n), taking the current condition of the plant into account. The value HEP_j^n can also be represented in the form of a typical repair rate expression, as below:

$$HEP_j^n = e^{-\mu_{r,j}^n \times \Delta T_{r(grace),j}} \tag{1}$$

where $\Delta T_{r(grace),j}$ is the grace period allowed for repairing the j_{th} SSC, and $\mu_{r,j}^n$ is the instantaneous repair rate at step n. By rearranging the equation, it becomes clear that $\mu_{r,j}^n$ reflects the effects of the current plant state as captured by HEP_j^n in the HRA.

$$\mu_{r,j}^n = -\ \ln(HEP_j^n)/\Delta T_{r(grace)} \tag{2}$$

In addition, $\mu_{r,j}^n$ indicates the likelihood of a repair occurring within a unit time interval, assuming no previous repair has been performed for that task; therefore, incorporating this updated $\mu_{r,j}^n$ into the transition matrix at the end of the Markov chain process (illustrated in Fig. 1) allows for the calculation of the j_{th} SSC's state transition probabilities (namely, the probability of switching to a working state ($P_{work,j}^{n+1}$) or staying in a malfunctioning state ($P_{mal,j}^{n+1}$) at the $n+1_{th}$ step) while factoring in the current state of the SSC. Here, if the j_{th} SSC is operational at step n, then $SSC_{work,j}^n = 1$ and $SSC_{mal,j}^n = 0$, and vice versa. Finally, Monte Carlo sampling is applied using $P_{work,j}^{n+1}$ and $P_{mal,j}^{n+1}$, allowing for the stochastic resolve of the j_{th} SSC's state at the $n+1_{th}$ step.

III. TEST CASE EXPLANATION

III.A. Applied Scenario

To examine the proposed CMMC-based framework, this study applies a hypothetical scenario involving volcanic ashfall on a typical sodium-cooled fast reactor (SFR), as illustrated in Fig. 2. In the SFR, decay heat removal depends on the Auxiliary Cooling System (ACS), which operates through air cooling. The ACS can function in either Forced Circulation (FC) or Natural Circulation (NC) mode; the FC mode requires power supplied by the Electricity Distribution System (EDS). However, volcanic ashfall may clog the ACS filters, potentially causing system failure. Furthermore, ash accumulation can also affect the filters within the Emergency Diesel Generators (EDGs) and the Heating, Ventilation, and Air Conditioning (HVAC) system. These effects ultimately influence whether the EDS can provide electricity to the ACS to enable FC mode operation.

To restore decay heat removal capability, repair tasks involve replacing the malfunctioning filters. During the replacement, the clogged ash on the filter would be disturbed, dislodged, and subsequently dispersed into the surrounding work environment, increasing airborne ash concentration. This elevated ash concentration reduces visibility for personnel, which may adversely affect the performance of repair tasks.

The analysis of filter malfunctions is conducted by the Malfunction Analysis Module within the SSCs States Solver, as shown in Fig. 1, where methodological details are available in previous work [2]. Therefore, this study primarily concentrates on the Repair Analysis Module related to filter replacement and illustrates how the HEP is dynamically updated in response to spatiotemporal environmental variations, as detailed in the following section.

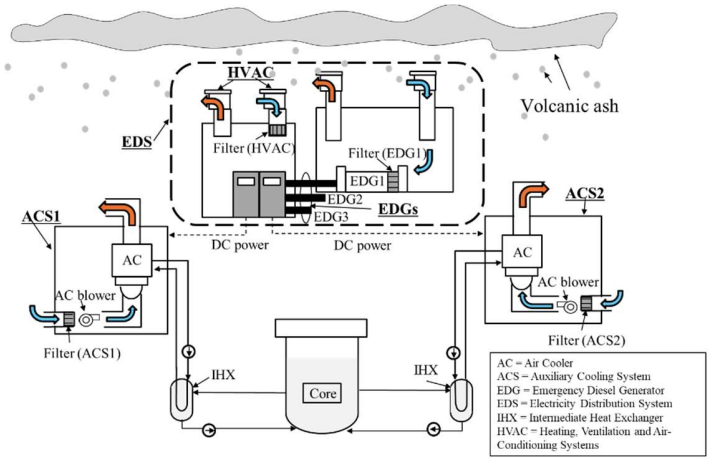

FIGURE 2. The schematic of interactions between the ACSs and adjacent components/systems under volcanic ashfall.

III.B. HEP Update

III.B.1. HEP Estimation

The concept underlying the estimation of HEP in this study is introduced here. First, a task structure analysis must be conducted. An example of such a task structure, represented by a Crew Response Diagram (CRD), is presented in Fig. 3.

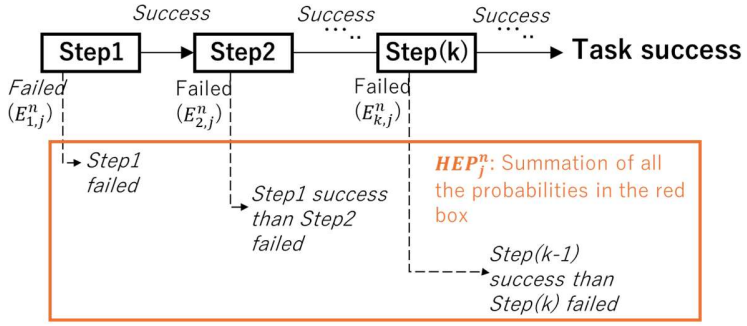

FIGURE 3. Example of task structure analysis via the Crew Response Diagram (CRD).

After conducting the task structure analysis and breaking down its constituent steps, the HEP for the j_{th} SSC at the n_{th} time step, denoted as HEP_j^n, can be expressed as follows:

$$HEP_j^n = 1 - \prod_{k=1}^{K}\left[1 - P\left(E_{k,j}^n \,\middle|\, (1 - E_{k-1,j}^n)\right)\right] \tag{3}$$

$$P\left(E_{k,j}^n \,\middle|\, (1 - E_{k-1,j}^n)\right) = \frac{d \times E_{k,j}^n}{d+1} \qquad [if\ k \neq 1] \tag{4}$$

$$P\left(E_{k,j}^n \,\middle|\, (1 - E_{k-1,j}^n)\right) = E_{1,j}^n \qquad [if\ k = 1] \tag{5}$$

where $E_{k,j}^n$ represents the human error probability for the k_{th} step at the n_{th} timestep for the j_{th} SSC. The parameter d in Eq. (4) accounts for the dependence level between consecutive steps (k_{th} and $k-1_{th}$) to model the conditional probability of $E_{k,j}^n$. Several factors influence this dependence level, including the similarity of equipment operated at each step, the time lag between step executions, and the spatial distance between operation locations. Additionally, the operator's skill proficiency plays a significant role. For the different dependence levels of complete dependence (CD), high dependence (HD), moderate dependence (MD), low dependence (LD), and zero dependence (ZD), d equal to 0, 1, 6, 19, and ∞, respectively. Furthermore, $E_{k,j}^n$ can be estimated using the following equation:

$$E_{k,j}^{n} = NHEP_{k,j}^{n} \times PSF_{j}^{n} \tag{6}$$

where $NHEP_{k,j}^{n}$ represents the nominal HEP, and PSF_{j}^{n} denotes the performance shaping factor for the k_{th} step at the n_{th} time step for the j_{th} SSC. In this research, PSF_{j}^{n} is further decomposed into the following components:

$$PSF_{j}^{n} = PSF_{base,j}^{n} \times PSF_{enviromen\ ,j}^{n} \tag{7}$$

where $PSF_{enviroment,j}^{n}$ represents the influence of dynamic environmental conditions, and $PSF_{base,j}^{n}$ accounts for all remaining contributions that are independent of environmental changes.

In this study, the repair task is assumed to consist of four sequential steps: (1) Loosen the screw, (2) Take-off the old filter, assuming LD with the former step (3) Install the new filter, assuming HD with the former step, and (4) Fasten the screw, assuming LD with the former step. Furthermore, the traditional HRA method, THERP, is employed as an example to estimate both the $NHEP_{k,j}^{n}$ and the $PSF_{base,j}^{n}$. The procedure for updating the $PSF_{enviroment,j}^{n}$ at each time step is detailed in the following section.

III.B.2. Update $PSF_{enviroment,j}^{n}$ in Response to Environmental Spatiotemporal Change

Based on the hypothetical repair task described in Section III.A, the update process of $PSF_{enviroment,j}^{n}$ at each time step in the Repair Analysis Module is divided into two stages: (1) estimating visibility according to changes in the volcanic ash concentration in the working environment, and (2) updating $PSF_{enviroment,j}^{n}$ based on the resulting changes in visibility.

Before estimating visibility, it is necessary to calculate the volcanic ash mass concentration in the working environment within the Plant State Solver (as illustrated in Fig. 1). This calculation accounts for the ash dislodged from the malfunctioning filter during the repair task. In this study, Fick's first law is applied to the continuity equation to model the diffusion process of the dislodged ash. Consequently, the spatiotemporal-dependent ash mass concentration, $c(r,t)$ [kg/m^3], is governed by the following equation:

$$\frac{\partial c(r,t)}{\partial t} = D\nabla^2 c(r,t) + S(r,t) \quad [r \in \mathbb{R}^3, t > 0] \tag{8}$$

where $\boldsymbol{D}$ [m^2/s] is diffusivity constant, and $\boldsymbol{S(r,t)}$ represents the source term for volcanic ash generation or absorption. Since the dislodged ash from the malfunctioning filter should be considered as $\boldsymbol{S(r,t)}$, a simplification is made by assuming that the dislodged ash is released instantaneously at the beginning of the task rather than continuously over time. Under this assumption, $\boldsymbol{S(r,t)}$ is set to zero, and the initial released ash mass concentration $\boldsymbol{M_0}$ [kg/m^2] around the released location $\boldsymbol{r_0}$ is defined as the initial condition. Meanwhile, at an infinite distance from the point of ash release, the ash concentration is assumed to be zero as the boundary condition. For a three-dimensional infinite domain, the classical analytical solution for $\boldsymbol{c(r,t)}$ under the given conditions is as below [3]:

$$c(r,t) = \frac{M_0}{(4\pi Dt)^{1/2}} e^{\left(\frac{-\|r-r_0\|^2}{4Dt}\right)} \quad [t > 0] \tag{9}$$

In this study, $\boldsymbol{r_0}$ is set as 0. Furthermore, considering the repetitive nature of the repair task, the contribution of all previously released ash masses can be treated as a linear superposition. Consequently, the expression for $\boldsymbol{c(r,t)}$ is expanded to:

$$c_j^n = \sum_{M=1}^{m} H(t_j^n - t_{j,M(start)}) \times \frac{M_{j,M}}{[4\pi D(t_j^n - t_{j,M(start)})]^{1/2}} \times e^{\left(\frac{-\|r_j^n\|^2}{4D(t_j^n - t_{j,M(start)})}\right)} \tag{10}$$

where c_j^n [kg/m^3] means the ash mass concentration when repairing j_{th} component at n_{th} timestep, and $t_{j,M(start)}$ [s] means the starting time of the M_{th} repair task for j_{th} component, and m means the order of the current task when repairing j_{th} SSC at n_{th} timestep. $H(\cdot)$ is the Heaviside step function ensuring that contributions from previous repair tasks are only considered when $t_j^n > t_{j,M(start)}$. $M_{j,M}$ [kg/m^2] is the released ash mass concentration from the M_{th} repair task. By setting the radial distance between the dislodged ash and the staff position as r_j^n[m], c_j^n at each timestep can be determined by using Eq. (10) within Plant State Solver.

Once the Plant State Solver calculates c_j^n, this information is transferred to the Repair Analysis Module within the SSCs States Solver to assess the impact of c_j^n on the visibility. Visibility is typically expressed as follows:

$$V_j^n = 3.912/\beta_{ext,j}^n \tag{11}$$

where V_j^n [m] denotes the visibility distance during the repair of the j_{th} component at the n_{th} timestep, and $\beta_{ext,j}^n$ [1/m] represents the extinction coefficient corresponding to c_j^n. When the diameter of the volcanic ash particles is significantly larger than the wavelength of visible light, the geometric scattering approximation can be applied [4], allowing $\beta_{ext,j}^n$ to be expressed as follows:

$$\beta_{ext,j}^n = 2\pi \sum_i r_i^2 n_j^n(r_i) \tag{12}$$

where $\boldsymbol{n_j^n(r_i)}$ [1/m^3] denotes the number density of ash particles with radius $\boldsymbol{r_i}$ during the repair of the j_{th} component at the n_{th} timestep. Accordingly, the impact of ash mass concentration on $\boldsymbol{V_j^n}$ can be estimated by applying the information of $\boldsymbol{c_j^n}$ from Eq. (10) to $\sum_i \boldsymbol{r_i^2 n_j^n(r_i)}$ in Eq. (12). Then, in this study, when $\boldsymbol{V_j^n}$ decreases to less than one meter, the $\boldsymbol{PSF_{enviroment,j}^n}$ is assumed to increase to a value of two. Moreover, the relationship between $\boldsymbol{PSF_{enviroment,j}^n}$ and $\boldsymbol{V_j^n}$ is modeled as an exponential decay function, as expressed in Eqs. (13) and (14).

$$PSF_{enviroment,j}^n = 1 + e^{2(1-V_j^n)} \qquad [if\ V_j^n \geq 1] \tag{13}$$

$$PSF_{enviromen\ ,j}^n = 2 \qquad [if\ V_j^n < 1] \tag{14}$$

III.C. Summary of the Case Explanation

This example demonstrates how transient environmental factors, exemplified by the dynamic evolution of ash concentration c_j^n, can be quantitatively linked to $PSF_{enviroment,j}^n$ in the context of updating HEP. Specifically, visibility V_j^n acts as an intermediary variable connecting environmental conditions with human performance. By embedding this mechanism within the proposed computational framework, transient environmental influences can be dynamically and bidirectionally integrated into HRA during repair tasks.

IV. RESULTS AND DISCUSSION

To further assess the framework's capability to bidirectionally respond to environmental spatiotemporal changes, an additional test case is introduced alongside the scenario described in Chapter III (hereafter referred to as AM1(DHRA)). This new case, named AM1 in the following discussion, fixes the value of $PSF_{enviroment,j}^n$ at one, thereby neglecting the influence of c_j^n. For each case, 500 samples are included in the analysis.

Fig. 4(a) illustrates an example of ACS state history for the AM1(DHRA) case. The y-axis represents the ACS states: forced circulation (value 2), natural circulation (value 1), and failure (value 0). Correspondingly, Fig. 4(b) depicts the temporal variation of ash concentration in the room housing the ACS, accounting for ash dislodged from the malfunctioning filter once repair operations commence following filter failure. Furthermore, Fig. 5 compares the ash concentration histories in alternative rooms containing different ACS units and EDGs. It is observed that the equilibrium room ash concentration increases with the number of repair tasks performed, indicating that the cumulative effects of prior repairs on the same component/system are considered. Additionally, the rate of increase in equilibrium room ash concentration is more pronounced in EDG environments than in ACS, owing to the higher repair frequency of EDGs, which stems from their greater inflow rates [2] and consequently leads to higher failure rates compared to ACS units.

Subsequently, two indices are employed to evaluate the analytical results of AM1(DHRA) and AM1 from the perspectives of heat removal ability (Index 1, presented in Fig. 6(a)) and repair cost (Index 2, shown in Fig. 6(b)). The definitions of Index 1 and Index 2 are provided below:

$$Index1 = \frac{0.5\times(t_{ACS1-} + t_{ACS2-}) + 0.25\times(t_{ACS1-} + t_{ACS2-})}{24\ hours} \tag{15}$$

$$Index2 = t_{repai} \times n_{staff\ per\ repair} \tag{16}$$

where t_{ACS1-} represents the total operating time of ACS1 in forced circulation mode in a sample, t_{re} denotes the total repair time for all filters in a sample, and $n_{staff\ per\ repair}$ corresponds to the number of staff assigned to perform a repair task (three staff members in this study). An Index 1 value of one indicates that both ACS1 and ACS2 operated continuously in FC mode over the past 24 hours. As shown in Fig. 6(a), incorporating dynamic HRA that accounts for environmental spatiotemporal changes during repair task analysis shows a detrimental effect on decay heat removal capability.

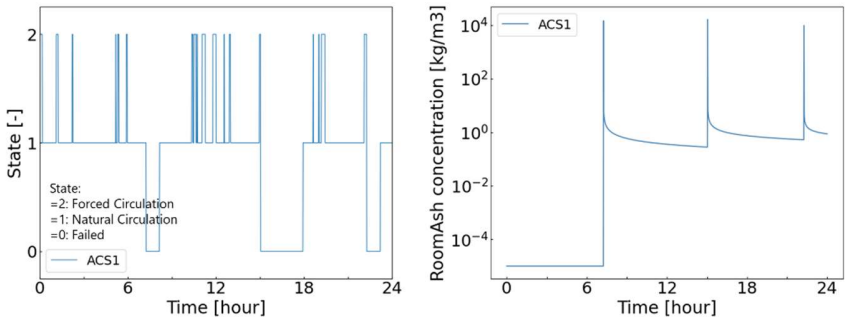

FIGURE 4. A sample of considering the environmental spatiotemporal change on the repair task: (a) ACS's state history, and (b) historical data of the ash concentration in the room housing ACS1.

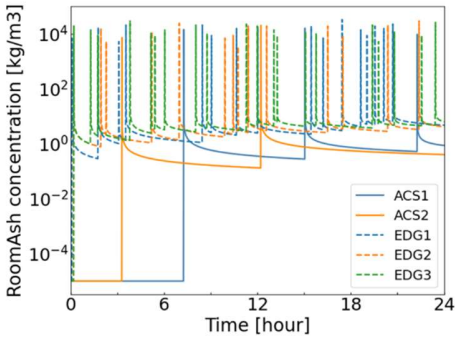

FIGURE 5. Historical data of the ash concentration in the room housing different components/systems.

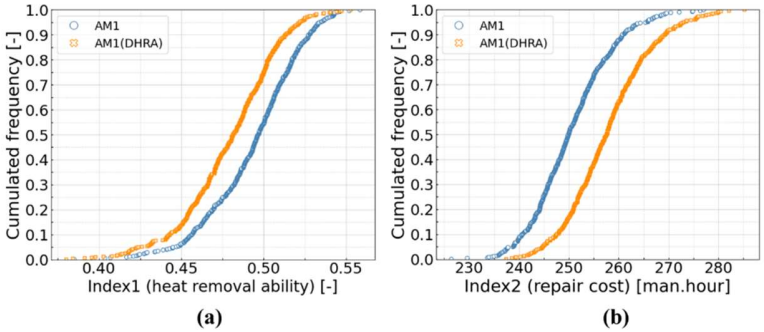

FIGURE 6. The cumulated frequency to Index 1 (heat removal ability) and Index 2 (repair cost) among different cases, including w/o considering the environmental spatiotemporal change on the repair task.

To further explore the factors contributing to the differences in Index 1 between the cases, Fig. 7(a) shows that the average repair time for an ACS filter is longer in the AM1(DHRA) case. This increase is attributed to the reduced visibility caused by ash dislodged from repeatedly replaced malfunctioning filters, as reflected in the dynamic updating of HEP within the Repair Analysis Module. Concurrently, the longer average repair time reduces the frequency of ACS repairs, as depicted in Fig. 7(b), resulting in only a slightly higher total ACS repair time in AM1(DHRA) compared to AM1 (Fig. 7(c)). This is consistent with the marginally lower total ACS operating time observed in AM1(DHRA) (Fig. 7(d)). However, since the failure frequency of

EDGs is higher than that of ACS units, the reduction in operating time is more pronounced for EDGs when environmental spatiotemporal changes are considered in repair task analysis. Therefore, as shown in Fig. 7(e), the ratio of operating time in FC mode to total operating time is significantly lower in AM1(DHRA), indicating that the FC-to-total time ratio is a more critical factor influencing heat removal capability (Index 1) than total operating time alone (Fig. 7(d)). Finally, the relationship between Index 1 and Index 2, presented in Fig. 7(f), reveals that economic efficiency related to repair tasks tends to be overestimated if the influence of environmental spatiotemporal changes is neglected.

In summary, these results demonstrate the capability of the proposed CMMC-based framework to quantitatively capture the uncertainties arising from bidirectional environmental spatiotemporal changes on repair task analysis from multiple perspectives, including heat removal performance and economic efficiency. Moreover, the framework facilitates intuitive investigation and identification of key factors influencing the defined indices.

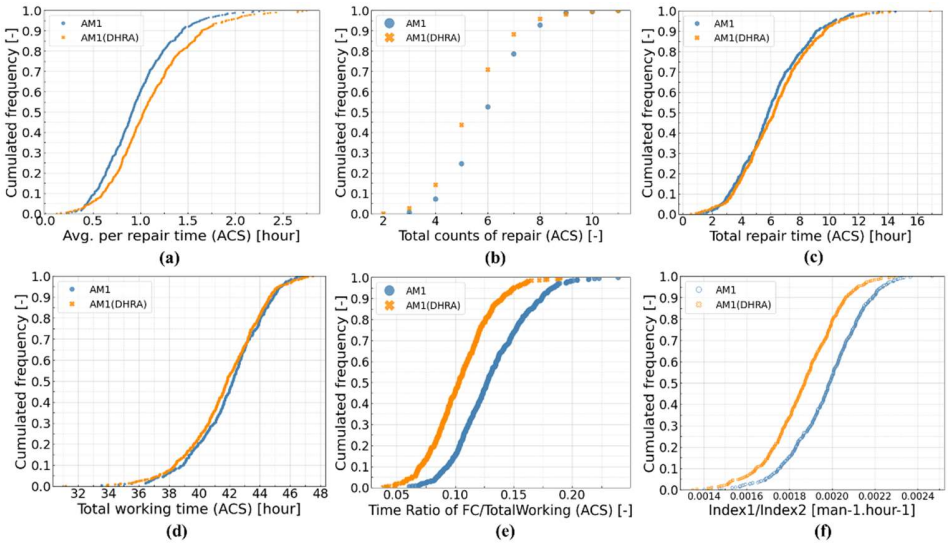

FIGURE 7. The cumulated frequency to the parameters related to the Index 1 investigation among different cases.

V. CONCLUSIONS

To realize dynamic HRA, this study proposes a computational framework that integrates the CMMC method. In summary, the framework demonstrates the following key features: (1) incorporating and quantifying the effects of environmental spatiotemporal variations on human behavior through the Markov chain process within the CMMC method; (2) translating changes in human behavior into dynamic events that provide feedback to the evolving environment via Monte Carlo sampling; and (3) enabling bidirectional dynamic interactions between humans and the environment within the developed computational framework. Additionally, an example application of the proposed framework is presented to illustrate its potential in quantitatively capturing uncertainties arising from environmental spatiotemporal influences on repair task analysis. However, the current stage of this study is limited to the case of filter replacement in response to volcanic ashfall hazards, and the relationship between visibility in the working environment and PSFs still requires further investigation. Future work will focus on conducting additional case studies to validate and expand the applicability of the proposed framework.

REFERENCES

[1] A. D. Swain and H. E. Guttmann, *Handbook of human-reliability analysis with emphasis on nuclear power plant applications. Final report*, NUREG/CR-1278, U.S. (1983).

[2] C. Y. Li, A. Watanabe, A. Uchibori and Y. Okano, "The development of petri net-based continuous Markov chain Monte Carlo methodology applying to dynamic probability risk assessment for multi-state resilience systems with repairable multi-component interdependency under longtermly thereat," *Journal of Nuclear Science and Technology*, **61** (7), pp. 935-957 (2024).

[3] "Chapter 2 Fickian Diffusion," *https://ocw.snu.ac.kr/node/14445/* (2018).

[4] C. H. Jung and Y. P. Kim, "Particle Extinction Coefficient for Polydispersed Aerosol Using a Harmonic Mean Type General Approximated Solution," *Aerosol Science and Technology*, **41** (11), pp. 994-1001 (2007).